The Generalized Brain-State-in-a-Box (gBSB) Neural Network: Model, Analysis, and Applications

Cheolhwan Oh and Stanislaw H. Żak
School of Electrical and Computer Engineering
Purdue University
West Lafayette, IN 47907, USA
Email: {oh2, zak}@purdue.edu

Stefen Hui
Department of Mathematical Sciences
San Diego State University
San Diego, CA 92182, USA
Email: hui@saturn.sdsu.edu

***Abstract*— The generalized Brain-State-in-a-Box (gBSB) neural network is a generalized version of the Brain-State-in-a-Box (BSB) neural network. The BSB net is a simple nonlinear autoassociative neural network that was proposed by J. A. Anderson, J. W. Silverstein, S. A. Ritz, and R. S. Jones in 1977 as a memory model based on neurophysiological considerations. The BSB model gets its name from the fact that the network trajectory is constrained to reside in the hypercube $H_n = [-1, 1]^n$. The BSB model was used primarily to model effects and mechanisms seen in psychology and cognitive science. It can be used as a simple pattern recognizer and also as a pattern recognizer that employs a smooth nearness measure and generates smooth decision boundaries. Three different generalizations of the BSB model were proposed by Hui and Żak, Golden, and Anderson. In particular, the network considered by Hui and Żak, referred to as the generalized Brain-State-in-a-Box (gBSB), has the property that the network trajectory constrained to a hyperface of H_n is described by a lower-order gBSB type model. This property simplifies significantly the analysis of the dynamical behavior of the gBSB neural network. Another tool that makes the gBSB model suitable for constructing associative memory is the stability criterion of the vertices of H_n. Using this criterion, a number of systematic methods to synthesize associative memories were developed.**

In this paper, an introduction to some useful properties of the gBSB model and some applications of this model are presented first. In particular, the gBSB based hybrid neural network for storing and retrieving pattern sequences is described. The hybrid network consists of autoassociative and heteroassociative parts. In the autoassociative part, where patterns are usually represented as vectors, a set of patterns is stored by the neural network. A distorted (noisy) version of a stored pattern is subsequently presented to the network and the task of the neural network is to retrieve (recall) the original stored pattern from the noisy pattern. In the heteroassociative part, an arbitrary set of input patterns is paired with another arbitrary set of output patterns. After presenting hybrid networks, neural associative memory that processes large scale patterns in an efficient way is described. Then the gBSB based hybrid neural network and the pattern decomposition concept are used to construct a neural associative memory. Finally, an image storage and retrieval system is constructed using the subsystems described above. Results of extensive simulations are included to illustrate the operation of the proposed image storage and retrieval system.

I. Introduction

James A. Anderson, a pioneer in the area of artificial neural networks, writes in [1, page 143]: "most memory in humans is associative. That is, an event is linked to another event, so that presentation of the first event gives rise to the linked event." An associative memory may be considered a rudimentary model of human memory. In general, a memory that can be accessed by the storage address is called an address addressable memory (AAM) and a memory that can be accessed by content is called a content addressable memory (CAM) or an associative memory. When an associative memory is constructed using a dynamical system, it is called a neural associative memory. Associative memories can be classified into two types: autoassociative and heteroassociative memories. In an autoassociative memory, after prototype patterns are stored by a neural network, where patterns are usually represented as vectors, a distorted (noisy) version of a stored pattern is subsequently presented to the network. The task of the neural associative memory is to retrieve (recall) the original stored pattern from its noisy version. Another type of associative memory is a heteroassociative memory, where a set of input patterns is paired with a different set of output patterns. Operation of a neural associative memory is characterized by two stages: storage phase, where patterns are being stored by the neural network, and recall phase, where memorized patterns are being retrieved in response to a noisy pattern being presented to the network. In this paper, we present in a tutorial fashion, the generalized Brain-State-in-a-Box (gBSB) neural network that is suitable for construction of associative memories, and then present dynamical properties of gBSB model and its applications. For other neural associative memory models see, for example, [2], [3], [4], [5], [6], [7], [8].

The paper is organized as follows. In Section II, we introduce the Brain-State-in-a-Box (BSB) neural model. In Section III, we analyze useful properties of the gBSB neural network. In Section IV, we present a method to construct associative memory using the gBSB neural network. In Section V, we offer a method for designing large scale neural associative memory using overlapping decomposition, and show the simulation results of image storage and retrieval. In Section VI, we propose a neural system that can store and retrieve pattern sequences, and present an application to the image storage and retrieval. Conclusions are found in Section VII. Finally, possible research projects are listed in Section VIII.

II. Brain-State-in-a-Box (BSB) Neural Network

The Brain-State-in-a-Box (BSB) neural network is a simple nonlinear autoassociative neural network that was proposed by J. A. Anderson, J. W. Silverstein, S. A. Ritz, and R. S. Jones in 1977 [9] as a memory model based on neurophysiological considerations. The BSB model gets its name from the fact that the network trajectory is constrained to reside in the hypercube $H_n = [-1,1]^n$. The BSB model was used primarily to model effects and mechanisms seen in psychology and cognitive science [1]. A possible function of the BSB net is to recognize a pattern from a given noisy version. The BSB net can also be used as a pattern recognizer that employs a smooth nearness measure and generates smooth decision boundaries [10]. The dynamics of the BSB model and its modified models were analyzed by Greenberg [11], Golden [12], [13], Grossberg [14], Hui and Żak [15], Hakl [16], Hui, Lillo, and Żak [17], Lillo et al. [18], Anderson [1], Perfetti [19], Hassoun [20], Żak, Lillo, and Hui [21], Chan and Żak [22], [23], Park, Cho, and Park [24]. A continuous counterpart of the BSB model referred to as the linear system operating in a saturated mode was analyzed in Li, Michel, and

Porod [25]. We next introduce the concept of linear associative memory to prepare us for a discussion of neural associative memories.

A. Linear associative memory

We use a simple linear associative memory to illustrate the concept of associative memory. Suppose that r mutally orthogonal patterns $\boldsymbol{v}^{(j)}, j = 1, 2, \ldots, r$, $\boldsymbol{v}^{(i)T}\boldsymbol{v}^{(j)} = 0$ for $i \neq j$, are to be stored in a memory. Let $\boldsymbol{V} = [\boldsymbol{v}^{(1)}\ \boldsymbol{v}^{(2)}\ \cdots\ \boldsymbol{v}^{(r)}]$ and let

$$\boldsymbol{W} = \sum_{j=1}^{r} \boldsymbol{v}^{(j)}\boldsymbol{v}^{(j)T} = \boldsymbol{V}\boldsymbol{V}^T,$$

where $\boldsymbol{V}^T$ denotes the transpose of $\boldsymbol{V}$. Consider the simple linear system

$$\boldsymbol{y} = \boldsymbol{W}\boldsymbol{x}.$$

If an input presented to the system is one of the stored patterns, that is, $\boldsymbol{x} = \boldsymbol{v}^{(k)}, k \in \{1, 2, \ldots, r\}$, then

$$\begin{aligned} \boldsymbol{y} = \boldsymbol{W}\boldsymbol{v}^{(k)} &= \sum_{j=1}^{r} \boldsymbol{v}^{(j)}\boldsymbol{v}^{(j)T}\boldsymbol{v}^{(k)} \\ &= \boldsymbol{v}^{(k)}\boldsymbol{v}^{(k)T}\boldsymbol{v}^{(k)} = c\boldsymbol{v}^{(k)}, \end{aligned}$$

where $c = \boldsymbol{v}^{(k)T}\boldsymbol{v}^{(k)}$. Thus, we obtained the input pattern as the output of the system. The above is an example of an autoassociative memory.

Now, let us consider the case when the input to the system is a portion of a stored pattern. The following example is from [26]. Let

$$\boldsymbol{v}^{(k)} = \boldsymbol{v}^{(k1)} + \boldsymbol{v}^{(k2)}$$

and assume that $\boldsymbol{v}^{(k1)}$ and $\boldsymbol{v}^{(k2)}$ are orthogonal to each other and that $\boldsymbol{v}^{(k1)}$ is orthogonal to $\boldsymbol{v}^{(1)}, \ldots, \boldsymbol{v}^{(k-1)}, \boldsymbol{v}^{(k+1)}, \ldots, \boldsymbol{v}^{(r)}$. If the input of the system is $\boldsymbol{x} = \boldsymbol{v}^{(k1)}$, then

$$\begin{aligned} \boldsymbol{y} &= \boldsymbol{W}\boldsymbol{v}^{(k1)} \\ &= \sum_{j=1}^{r} \boldsymbol{v}^{(j)}\boldsymbol{v}^{(j)T}\boldsymbol{v}^{(k1)} \\ &= \boldsymbol{v}^{(k)}\boldsymbol{v}^{(k)T}\boldsymbol{v}^{(k1)} \\ &= (\boldsymbol{v}^{(k1)} + \boldsymbol{v}^{(k2)})(\boldsymbol{v}^{(k1)} + \boldsymbol{v}^{(k2)})^T\boldsymbol{v}^{(k1)} \\ &= (\boldsymbol{v}^{(k1)} + \boldsymbol{v}^{(k2)})\boldsymbol{v}^{(k1)T}\boldsymbol{v}^{(k1)} \\ &= d\boldsymbol{v}^{(k)}, \end{aligned}$$

where $d = \boldsymbol{v}^{(k1)T}\boldsymbol{v}^{(k1)}$. Therefore, the linear associator recovered the original stored pattern from the partial input, that is, the linear associator is an example of the CAM. A limitation of the above system is that when the patterns are not orthogonal to each other, it does not retrieve the stored pattern correctly. Also, when the input vector is a noisy version of the prototype pattern, the linear associator above is not able to recall the corresponding prototype pattern.

Next, we introduce the Brain-State-in-a-Box (BSB) neural network that can be used as an associative memory. The BSB net can retrieve a certain pattern when its noisy version is presented as an input to the net.

B. Brain-State-in-a-Box (BSB) neural network model

The dynamics of the BSB neural network are described by the difference equation,

$$\boldsymbol{x}(k+1) = \boldsymbol{g}(\boldsymbol{x}(k) + \alpha\boldsymbol{W}\boldsymbol{x}(k)), \qquad (1)$$

with an initial condition $\boldsymbol{x}(0) = \boldsymbol{x}_0$, where $\boldsymbol{x}(k) \in \mathbb{R}^n$ is the state of the BSB neural network at time k, $\alpha > 0$ is a step size, $\boldsymbol{W} \in \mathbb{R}^{n\times n}$ is a symmetric weight matrix, and $\boldsymbol{g} : \mathbb{R}^n \to \mathbb{R}^n$ is an activation function defined as a standard linear saturation function,

$$(\boldsymbol{g}(\boldsymbol{x}))_i = (\boldsymbol{sat}(\boldsymbol{x}))_i = \begin{cases} 1 & \text{if} \quad x_i \geq 1 \\ x_i & \text{if} \quad -1 < x_i < 1 \\ -1 & \text{if} \quad x_i \leq -1. \end{cases} \qquad (2)$$

Figure 1 shows sample trajectories of the BSB model with the weight matrix

$$\boldsymbol{W} = \begin{bmatrix} 1.2 & -0.4 \\ -0.4 & 1.8 \end{bmatrix}. \qquad (3)$$

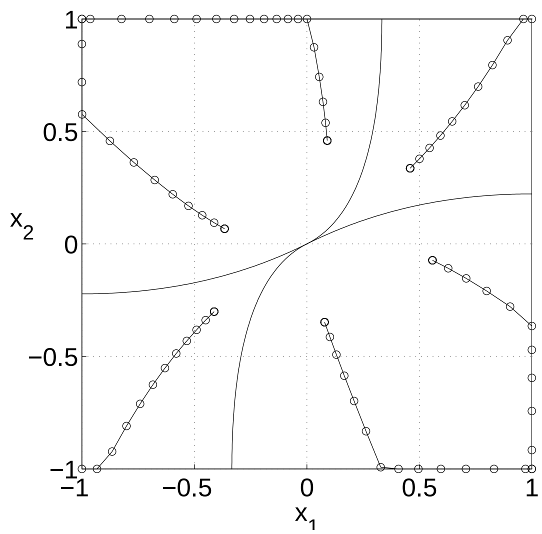

Fig. 1: Trajectories of the BSB model with the weight matrix (3).

The symmetric weight matrix of the BSB net is not desirable for the design of associative memory. Also, the ability to control the basins of attraction of the stable states is another property that makes it easier to design associative memory. Hui and Żak [15] devised a neural model that has the above properties, which is described in the following section.

III. Generalized Brain-State-in-a-Box (gBSB) Neural Network

Three different generalizations of the BSB model were proposed by Hui and Żak [15], Golden [13], and Anderson [1]. In particular, the network considered in [15], referred to as the generalized Brain-State-in-a-Box (gBSB), has the property that the network trajectory constrained to a hyperface of H_n is described by a lower-order gBSB type model. This interesting property simplifies significantly the analysis of the dynamical behavior of the gBSB neural network. Another tool that makes the gBSB model suitable for constructing associative memory is the stability criterion of the vertices of H_n proposed in [15]—see also [20] and [26] for further discussion of the condition. Lillo et al. [18] proposed a systematic method to synthesize associative memories using the gBSB neural network. This method is presented in this paper. For further discussion of the method to synthesize associative memories using the gBSB neural network, we refer the reader to [24], [27], and [28].

A. Model

The gBSB neural network allows for a nonsymmetrical weight matrix as well as to offer more control of the volume of the basins of attraction of the equilibrium states. The dynamics of the gBSB neural network are described by

$$\boldsymbol{x}(k+1) = \boldsymbol{g}((\boldsymbol{I}_n + \alpha \boldsymbol{W})\boldsymbol{x}(k) + \alpha \boldsymbol{b}), \qquad (4)$$

where $\boldsymbol{g}$ is the standard linear saturation function defined in (2), $\boldsymbol{I}_n$ is an $n \times n$ identity matrix, $\boldsymbol{b} \in \mathbb{R}^n$ is a bias vector, and the weight matrix $\boldsymbol{W} \in \mathbb{R}^{n\times n}$ is not necessarily symmetric, which makes it easier to implement associative memories when using the gBSB network.

B. Stability

In this section, we discuss stability conditions for the neural networks presented in the previous section. To proceed further, the following definitions are needed.

Definition 1: A point $\boldsymbol{x}_e$ is an equilibrium state of the dynamical system $\boldsymbol{x}(k+1) = \boldsymbol{T}(\boldsymbol{x}(k))$ if $\boldsymbol{x}_e = \boldsymbol{T}(\boldsymbol{x}_e)$.

Definition 2: A basin of attraction of an equilibrium state of the system $\boldsymbol{x}(k+1) = \boldsymbol{T}(\boldsymbol{x}(k))$ is the set of points such that the trajectory of this system emanating from any point in the set converges to the equilibrium state $\boldsymbol{x}_e$.

In this section, we will be concerned with the equilibrium states that are vertices of the hypercube $H_n =$

$[-1, 1]^n$. That is, equilibrium points that belong to the set $\{-1, 1\}^n$.

Definition 3: An equilibrium point $\boldsymbol{x}_e$ of $\boldsymbol{x}(k+1) = \boldsymbol{T}(\boldsymbol{x}(k))$ is stable if for every $\epsilon > 0$ there is a $\delta = \delta(\epsilon) > 0$ such that if $\|\boldsymbol{x}(0) - \boldsymbol{x}_e\| < \delta$ then $\|\boldsymbol{x}(k) - \boldsymbol{x}_e\| < \epsilon$ for all $k \geq 0$, where $\|\cdot\|$ may be any p-norm of a vector, for example the Euclidean norm $\|\cdot\|_2$.

Definition 4: An equilibrium state $\boldsymbol{x}_e$ is super stable if there exists a neighborhood of $\boldsymbol{x}_e$, denoted $N(\boldsymbol{x}_e)$, such that for any initial state $\boldsymbol{x}_0 \in N(\boldsymbol{x}_e)$, the trajectory starting from $\boldsymbol{x}_0$ reaches $\boldsymbol{x}_e$ in a finite number of steps.

Let

$$\boldsymbol{L}(\boldsymbol{x}) = (\boldsymbol{I}_n + \alpha \boldsymbol{W})\boldsymbol{x} + \alpha \boldsymbol{b}$$

and let $(\boldsymbol{L}(\boldsymbol{x}))_i$ be the i-th component of $(\boldsymbol{L}(\boldsymbol{x}))$. Let $\boldsymbol{v} = \begin{bmatrix} v_1 & \cdots & v_n \end{bmatrix}^T \in \{-1, 1\}^n$, that is, $\boldsymbol{v}$ is a vertex of the hypercube H_n. For a vertex $\boldsymbol{v}$ to be an equilibrium point of the gBSB neural network, we must have

$$v_i = (\boldsymbol{g}(\boldsymbol{L}(\boldsymbol{v})))_i, \quad i = 1, \ldots, n.$$

That is, if $v_i = 1$, then we must have $(\boldsymbol{L}(\boldsymbol{v}))_i \geq 1$, and if $v_i = -1$, we must have $(\boldsymbol{L}(\boldsymbol{v}))_i \leq -1$. Thus, we obtain the following theorem that can be found in [15].

Theorem 1: A vertex $\boldsymbol{v}$ of the hypercube H_n is an equilibrium point of the gBSB neural network if and only if

$$(\boldsymbol{L}(\boldsymbol{v}))_i v_i \geq 1, \quad i = 1, \cdots, n.$$

Using the fact that $v_i^2 = 1$ and $\alpha > 0$, we can restate Theorem 1 as follows [26].

Theorem 2: A vertex $\boldsymbol{v}$ of the hypercube H_n is an equilibrium point of the gBSB neural network if and only if

$$(\boldsymbol{W}\boldsymbol{v} + \boldsymbol{b})_i v_i \geq 0, \quad i = 1, \cdots, n.$$

The following theorem, from [17], gives a sufficient condition for a vertex of H_n to be a super stable equilibrium state.

Theorem 3: Let $\boldsymbol{v}$ be a vertex of the hypercube H_n. If

$$(\boldsymbol{L}(\boldsymbol{v}))_i v_i > 1, \quad i = 1, \cdots, n, \tag{5}$$

then $\boldsymbol{v}$ is a super stable equilibrium point of the gBSB neural model.

Proof Because $(\boldsymbol{L}(\boldsymbol{x}))_i x_i$ is a continuous function, there exists a neighborhood $N(\boldsymbol{v})$ about $\boldsymbol{v}$ such that

$$(\boldsymbol{L}(\boldsymbol{x}))_i x_i > 1, \quad i = 1, \cdots, n \quad \text{and} \quad \boldsymbol{x} \in N(\boldsymbol{v}).$$

Therefore, for any $\boldsymbol{x} \in N(\boldsymbol{v})$, we have

$$\boldsymbol{g}(\boldsymbol{L}(\boldsymbol{x})) = \boldsymbol{v},$$

which means that $\boldsymbol{v}$ is indeed a super stable equilibrium point. $\square$

The sufficiency condition for a pattern to be a super stable equilibrium state given in the above theorem is a main tool in the design of associative memories discussed in this paper. The above condition referred to as the vertex stability criterion by Hassoun [20, page 411] is also essential when designing gBSB based associative memories. We note that such a condition cannot be obtained for a sigmoidal type of activation function.

Using the fact that $v_i^2 = 1$ and $\alpha > 0$, we can restate Theorem 3 as follows [26].

Theorem 4: Let $\boldsymbol{v}$ be a vertex of the hypercube H_n. If

$$(\boldsymbol{W}\boldsymbol{v} + \boldsymbol{b})_i v_i > 0, \quad i = 1, \cdots, n, \tag{6}$$

then $\boldsymbol{v}$ is a super stable equilibrium point of the gBSB neural model.

IV. Associative Memory Design Using gBSB Neural Network

In this section, we present a method of designing associative memory using gBSB neural networks. When the desired patterns are given, the associative memory should be able to store them as super stable equilibrium states of the neural net used to construct the associative memory. In addition, it is desirable to store the smallest number of spurious states as possible. We can synthesize gBSB based associative memories using the method proposed in [18]. We now briefly describe this method. For further discussion, see [26].

To proceed, we need the following definitions.

Definition 5: A matrix $\boldsymbol{D} \in \mathbb{R}^{n\times n}$ is said to be row diagonal dominant if

$$d_{ii} \geq \sum_{j=1, j\neq i}^{n} |d_{ij}|, \quad i = 1, \cdots, n.$$

It is strongly row diagonal dominant if

$$d_{ii} > \sum_{j=1, j\neq i}^{n} |d_{ij}|, \quad i = 1, \cdots, n.$$

Definition 6: Given $\boldsymbol{V} \in \mathbb{R}^{n\times r}$, a matrix $\boldsymbol{V}^{\dagger} \in \mathbb{R}^{r\times n}$ is called a pseudo-inverse of $\boldsymbol{V}$ if

1. $\boldsymbol{V}\boldsymbol{V}^{\dagger}\boldsymbol{V} = \boldsymbol{V}$;
2. $\boldsymbol{V}^{\dagger}\boldsymbol{V}\boldsymbol{V}^{\dagger} = \boldsymbol{V}^{\dagger}$;
3. $(\boldsymbol{V}\boldsymbol{V}^{\dagger})^T = \boldsymbol{V}\boldsymbol{V}^{\dagger}$;
4. $(\boldsymbol{V}^{\dagger}\boldsymbol{V})^T = \boldsymbol{V}^{\dagger}\boldsymbol{V}$.

Let $\boldsymbol{v}^{(1)}, \ldots, \boldsymbol{v}^{(r)}$ be given vertices of H_n that we wish to store as super stable equilibrium points of the gBSB neural network. We refer to these vertices as the prototype patterns. Then, we have the following theorem:

Theorem 5: Let

$$\boldsymbol{V} = \begin{bmatrix} \boldsymbol{v}^{(1)} & \cdots & \boldsymbol{v}^{(r)} \end{bmatrix} \in \{-1, 1\}^{n\times r}.$$

If

$$\boldsymbol{W} = \boldsymbol{D}\boldsymbol{V}\boldsymbol{V}^{\dagger},$$

where the matrix $\boldsymbol{D}$ satisfies

$$d_{ii} > \sum_{k=1, k\neq i}^{n} |d_{ik}| + |b_i|, \quad i = 1, \cdots, n, \tag{7}$$

then $\boldsymbol{v}^{(1)}, \ldots, \boldsymbol{v}^{(r)}$ are super stable points of the gBSB neural network.

Proof Using the property of the pseudo-inverse of $\boldsymbol{V}$, given in Definition 6, we obtain

$$\boldsymbol{W}\boldsymbol{V} = \boldsymbol{D}\boldsymbol{V}\boldsymbol{V}^{\dagger}\boldsymbol{V} = \boldsymbol{D}\boldsymbol{V}.$$

Therefore, for $j = 1, \ldots, r$, we have

$$\boldsymbol{W}\boldsymbol{v}^{(j)} = \boldsymbol{D}\boldsymbol{v}^{(j)}. \tag{8}$$

Combining (8) and (6) of Theorem 4, we obtain

$$\begin{aligned} &\left(\boldsymbol{W}\boldsymbol{v}^{(j)} + \boldsymbol{b}\right)_i v_i^{(j)} \\ &\quad = \left(\boldsymbol{D}\boldsymbol{v}^{(j)} + \boldsymbol{b}\right)_i v_i^{(j)} \\ &\quad = \left(d_{ii}v_i^{(j)} + \sum_{k=1, k\neq i}^{n} d_{ik}v_k^{(j)} + b_i\right) v_i^{(j)} \\ &\quad \geq d_{ii} - \sum_{k=1, k\neq i}^{n} |d_{ik}| - |b_i| \\ &\quad > 0. \end{aligned}$$

By Theorem 4, $\boldsymbol{v}^{(j)}$ is super stable. Note that the same argument holds for any $j = 1, \ldots, r$ and thus the proof is complete. $\square$

The above result is easy to apply when constructing the weight matrix $\boldsymbol{W}$. However, if the diagonal elements of the matrix $\boldsymbol{D}$ are too large, we may store all the vertices of the hypercube H_n, which is obviously not desirable.

The next theorem constitutes a basis for the weight matrix construction method.

Theorem 6: Let

$$\boldsymbol{V} = \begin{bmatrix} \boldsymbol{v}^{(1)} & \cdots & \boldsymbol{v}^{(r)} \end{bmatrix} \in \{-1, 1\}^{n\times r}$$

be the matrix of the prototype patterns, where $r < n$. Suppose the prototype patterns are linearly independent so that rank$(\boldsymbol{V}) = r$. Let $\boldsymbol{B} = \begin{bmatrix} \boldsymbol{b} & \cdots & \boldsymbol{b} \end{bmatrix} \in \mathbb{R}^{n\times r}$ be a matrix consisting of the column vector $\boldsymbol{b}$ repeated r times. Let $\boldsymbol{I}_n$ be the $n \times n$ identity matrix and let $\boldsymbol{\Lambda} \in \mathbb{R}^{n\times n}$. Suppose that $\boldsymbol{D} \in \mathbb{R}^{n\times n}$ is strongly row diagonal dominant, that is,

$$d_{ii} > \sum_{k=1, k\neq i}^{n} |d_{ik}|, \quad i = 1, \cdots, n.$$

If

$$\boldsymbol{W} = (\boldsymbol{D}\boldsymbol{V} - \boldsymbol{B})\boldsymbol{V}^{\dagger} + \boldsymbol{\Lambda}(\boldsymbol{I}_n - \boldsymbol{V}\boldsymbol{V}^{\dagger}), \qquad (9)$$

then all the patterns $\boldsymbol{v}^{(j)}, j = 1, \ldots, r$, are stored as super stable equilibrium points of the gBSB neural network.

Proof Because $\boldsymbol{V}^{\dagger}\boldsymbol{V} = \boldsymbol{I}_r$, we have

$$\boldsymbol{W}\boldsymbol{V} = \boldsymbol{D}\boldsymbol{V} - \boldsymbol{B},$$

or

$$\boldsymbol{W}\boldsymbol{v}^{(j)} = \boldsymbol{D}\boldsymbol{v}^{(j)} - \boldsymbol{b}, \quad j = 1, \ldots, r.$$

Therefore,

$$\begin{aligned}
\left(\boldsymbol{W}\boldsymbol{v}^{(j)} + \boldsymbol{b}\right)_i v_i^{(j)} &= \left(\boldsymbol{D}\boldsymbol{v}^{(j)} - \boldsymbol{b} + \boldsymbol{b}\right)_i v_i^{(j)} \\
&= \left(\boldsymbol{D}\boldsymbol{v}^{(j)}\right)_i v_i^{(j)} \\
&= d_{ii} + \sum_{k=1, k\neq i}^{n} d_{ik} v_k^{(j)} v_i^{(j)} \\
&\geq d_{ii} - \sum_{k=1, k\neq i}^{n} |d_{ik}| \\
&> 0.
\end{aligned}$$

Hence, by Theorem 4, each prototype pattern is a super stable equilibrium point of the gBSB neural network. □

For further analysis of the formula for the weight matrix synthesis given by (9), the reader is referred to [26, pp. 539–542].

The weight matrix construction algorithm is summarized in the following algorithm..

Algorithm 4.1: Weight matrix construction algorithm

1. For given prototype pattern vectors $\boldsymbol{v}^{(j)} \in \{-1, 1\}^n, j = 1, \ldots, r$, form a matrix $\boldsymbol{B} = \begin{bmatrix} \boldsymbol{b} & \boldsymbol{b} & \cdots & \boldsymbol{b} \end{bmatrix} \in \mathbb{R}^{n \times r}$, where

$$\boldsymbol{b} = \sum_{j=1}^{r} \epsilon_j \boldsymbol{v}^{(j)}, \quad \epsilon_j \geq 0, \quad j = 1, 2, \ldots r,$$

and ϵ_j's are design parameters.

2. Choose $\boldsymbol{D} \in \mathbb{R}^{n \times n}$ such that

$$d_{ii} > \sum_{j=1, j\neq i}^{n} |d_{ij}|, \quad \text{and}$$

$$d_{ii} < \sum_{j=1, j\neq i}^{n} |d_{ij}| + |b_i|, \quad i = 1, 2, \ldots, n,$$

and $\boldsymbol{\Lambda} \in \mathbb{R}^{n \times n}$ such that

$$\lambda_{ii} < -\sum_{j=1, j\neq i}^{n} |\lambda_{ij}| - |b_i|, \quad i = 1, 2, \ldots, n,$$

where d_{ij} and λ_{ij} are the ij-th elements of $\boldsymbol{D}$ and $\boldsymbol{\Lambda}$ respectively.

3. Determine the weight matrix $\boldsymbol{W}$ using the formula

$$\boldsymbol{W} = (\boldsymbol{D}\boldsymbol{V} - \boldsymbol{B})\boldsymbol{V}^{\dagger} + \boldsymbol{\Lambda}(\boldsymbol{I}_n - \boldsymbol{V}\boldsymbol{V}^{\dagger}),$$

where $\boldsymbol{V} = \begin{bmatrix} \boldsymbol{v}^{(1)} & \cdots & \boldsymbol{v}^{(r)} \end{bmatrix} \in \{-1, 1\}^{n \times r}$.

4. Implement an associative memory that can store the given patterns as super stable vertices of H_n using $\boldsymbol{W}$ and $\boldsymbol{b}$.

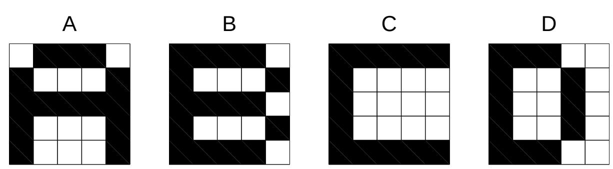

Fig. 2: Stored patterns.

We now illustrate the above algorithm with a simple example using a 25-dimensional gBSB net. We construct the weight matrix to store the four pattern vectors corresponding to the bitmaps shown in Figure 2. The elements of the bitmaps are either 1 (white) or -1 (black). The pattern vectors are obtained from the bitmaps by stacking their columns. For example, if $\boldsymbol{A} = \begin{bmatrix} \boldsymbol{a}_1 & \boldsymbol{a}_2 & \boldsymbol{a}_3 & \boldsymbol{a}_4 & \boldsymbol{a}_5 \end{bmatrix}$, where $\boldsymbol{a}_i, i = 1, \ldots, 5$, is the i-th column of $\boldsymbol{A}$, then the corresponding pattern vector is obtained from $\boldsymbol{A}$ by applying the stacking operator

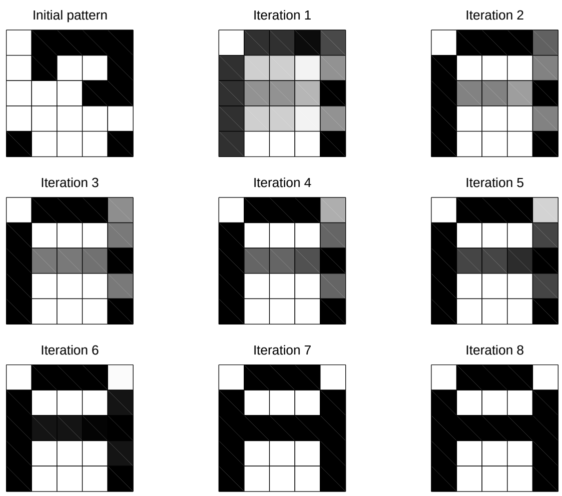

Fig. 3: Snapshots of a pattern that converges to a stored prototype pattern in the gBSB based neural associative memory.

$\boldsymbol{s} : \mathbb{R}^{5\times 5} \to \mathbb{R}^{25}$ to get

$$\boldsymbol{s}(\boldsymbol{A}) = \boldsymbol{A}(:) = \begin{bmatrix} \boldsymbol{a}_1 \\ \vdots \\ \boldsymbol{a}_5 \end{bmatrix} \in \{-1, 1\}^{25},$$

where $\boldsymbol{A}(:)$ is the MATLAB's command for the stacking operation on the matrix $\boldsymbol{A}$. The weight matrix, $\boldsymbol{W}$, was constructed using the above weight matrix construction algorithm, where

$$\boldsymbol{V} = \begin{bmatrix} \boldsymbol{A}(:) & \boldsymbol{B}(:) & \boldsymbol{C}(:) & \boldsymbol{D}(:) \end{bmatrix}.$$

In Figure 3, we show snapshots of the iterations converging towards the letter A of the gBSB neural network based associative memory.

The above method works well for small size patterns but is not suitable for large scale patterns. In the next section, we offer a technique that can effectively process large scale patterns.

V. Large Scale Associative Memory Design Using Overlapping Decomposition

In this section, we present a gBSB-based method to design neural associative memories that can process large scale patterns. A difficulty with large scale neural associative memory design is the quadratic growth of the number of interconnections with the pattern size, which results in a heavy computational load as the pattern size becomes large. To overcome this difficulty, we decompose large scale patterns into small size subpatterns to reduce the computational overhead. However, the recall performance of associative memories gets worse as the size of the neural associative memories is reduced. To alleviate this problem, we employ the overlapping decomposition method, which is used to provide the neural network with the capability of error detection. We discuss the overlapping decomposition method in some detail in the following subsection. The weight matrix of each subnetwork is determined by (9) independently of its neighboring subnetworks. We add the error detection and error correction features to our gBSB associative memory model, which successfully reduces the number of possible misclassifications. Other design approaches that use decomposition method can be found, for example, in [29], [30], [31].

A. Overlapping decomposition

To improve the capabilities of error detection and error correction and to process the subpatterns symmetrically, we propose two overlapping decompositions using a ring structure, suitable for vector patterns, and a toroidal structure that is suitable for images. We describe these two decomposition methods next. We begin by decomposing a pattern,

$$\boldsymbol{v} = \begin{bmatrix} v_1 \cdots & v_k & v_{k+1} & \cdots & v_{2k} & \cdots \\ & v_{(p-1)k+1} & \cdots & v_{pk} \end{bmatrix} \in \{-1, 1\}^{pk},$$

into p subpatterns,

$$\begin{aligned}
\boldsymbol{v}^{(1)} &= \begin{bmatrix} v_1 & \cdots & v_{k+1} \end{bmatrix} \in \{-1,1\}^{k+1}, \\
\boldsymbol{v}^{(2)} &= \begin{bmatrix} v_{k+1} & \cdots & v_{2k+1} \end{bmatrix} \in \{-1,1\}^{k+1}, \\
&\vdots \\
\boldsymbol{v}^{(p)} &= \begin{bmatrix} v_{(p-1)k+1} & \cdots & v_{pk} \end{bmatrix} \in \{-1,1\}^{k}.
\end{aligned}$$

Note that v_{k+1} is the overlapping element between $\boldsymbol{v}^{(1)}$ and $\boldsymbol{v}^{(2)}$, v_{2k+1} between $\boldsymbol{v}^{(2)}$ and $\boldsymbol{v}^{(3)}$, and so on. In this example, each subpattern except for $\boldsymbol{v}^{(1)}$ and $\boldsymbol{v}^{(p)}$ has two neighboring subpatterns and accordingly, has two overlapping elements. Each of $\boldsymbol{v}^{(1)}$ and $\boldsymbol{v}^{(p)}$ has only one overlapping element. Because the error detection scheme uses the overlapping elements between neighboring subnetworks, it is less likely to detect the errors for $\boldsymbol{v}^{(1)}$ and $\boldsymbol{v}^{(p)}$ than those for other subpatterns. However if we assume that the decomposition of the pattern $\boldsymbol{v}$ has a ring structure, $\boldsymbol{v}^{(1)}$ becomes another neighboring subpattern of $\boldsymbol{v}^{(p)}$, and vice versa. That is,

$$\boldsymbol{v}^{(p)} = \begin{bmatrix} v_{(p-1)k+1} & \cdots & v_{pk} & v_1 \end{bmatrix} \in \{-1,1\}^{k+1},$$

so that v_1 is the overlapping element between $\boldsymbol{v}^{(p)}$ and $\boldsymbol{v}^{(1)}$. In this decomposition, which we refer to as a ring overlapping decomposition, all subpatterns have the same dimensions.

We extend the above concept to the case when the patterns are represented by matrices, for example, images. An example of overlapping decomposition of a matrix pattern is shown in Figure 4. In Figure 4, the original pattern is decomposed so that there exist overlapping parts between neighboring subpatterns.

B. Associative memory with error correction unit

Large scale vector prototype patterns are decomposed into subpatterns with the ring overlapping decomposition while images are decomposed using the toroidal overlapping decomposition method. Then, the corresponding individual subnetworks are constructed employing the

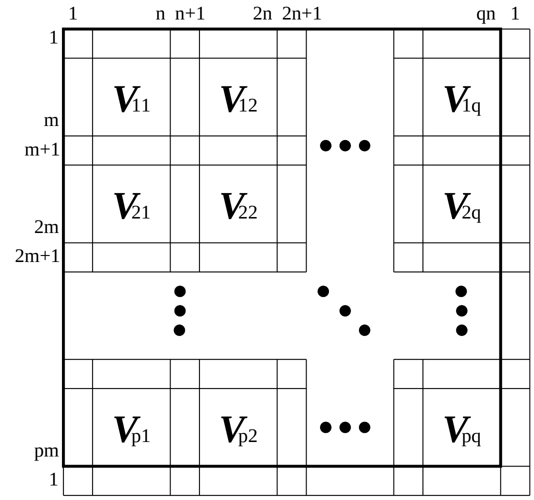

Fig. 4: An example of toroidal overlapping decomposition.

method in Section IV independently of other subnetworks. Each subpattern is assigned to a corresponding subnetwork as an initial condition. Then, each subnetwork starts processing the initial subpattern. After all the individual subnetworks have processed their subpatterns, the overlapping portions between adjacent subpatterns are checked. If the recall process is completed perfectly, all the overlapping portions of the subpatterns processed by the corresponding subnetworks should match. If a mismatched boundary is found between two adjacent subpatterns, we conclude that a recall error occurred in at least one of the two neighboring subnetworks during the recall process. In other words, the network has detected a recall error. Once an error is detected, the error correction algorithm is used to correct the recall errors. We next describe a procedure for the case of toroidal overlapping decomposition. The case of ring overlapping decomposition is described in [32].

Suppose we are processing an image. Then, every subpattern overlaps with four neighboring subpatterns in the decomposition shown in Figure 4. After the recall process, we check the number of mismatches

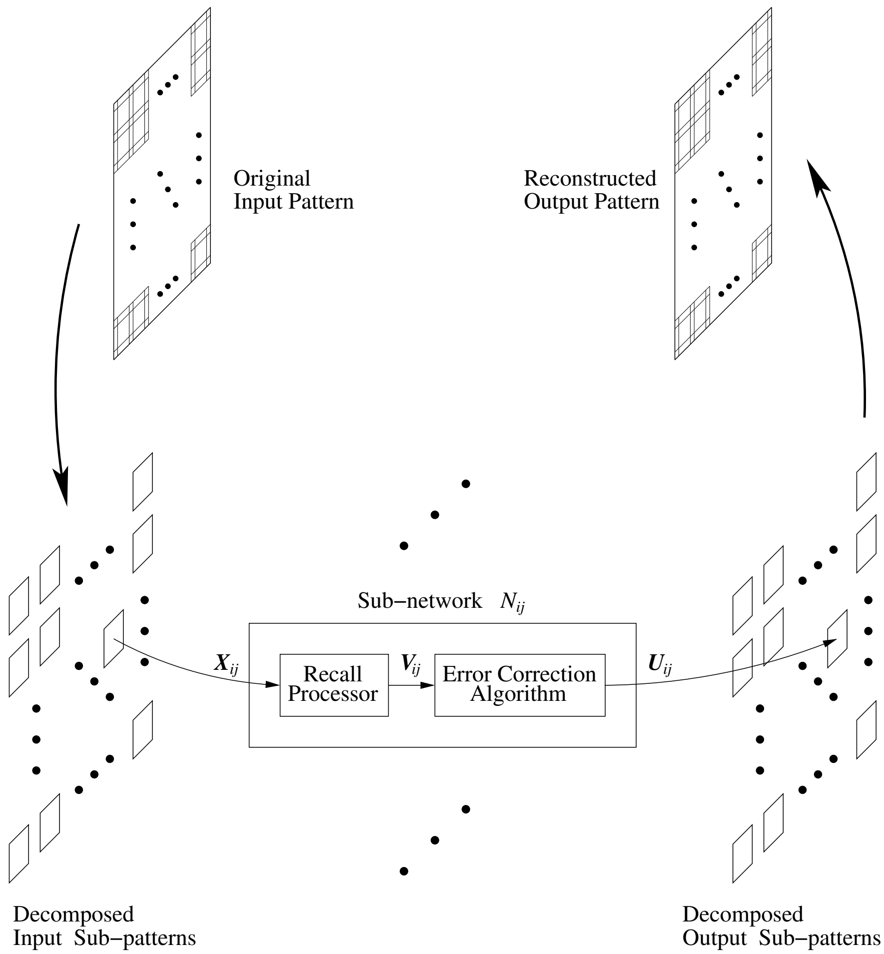

Fig. 5: Recall procedure using gBSB-based large scale associative memory with overlapping decompositions and error correction algorithm when the patterns are in the form of matrices, for example, images.

of the overlapping portions for each subpattern. We record the number of overlapping portions in which mismatches occur for each subpattern. The number of mismatched overlapping portions is an integer from the set $\{0, 1, 2, 3, 4\}$. We first check if there are subpatterns with no mismatches. If such a pattern is found, the algorithm is initiated by locating a marker on the above subpattern and then the marker moves horizontally to the next subpattern in the same row until a subpattern with mismatches is encountered. If all subpatterns have mismatches, we select a subnetwork with the minimal number of mismatches. Suppose the marker is located on the subnetwork N_{ij}, and assume that the right and the bottom portions of $\boldsymbol{V}_{ij}$ have mismatches. Note that the decomposed input pattern corresponding to the subnetwork N_{ij} is denoted $\boldsymbol{X}_{ij}$. We denote by $\boldsymbol{V}_{ij}$ the result of the recall process—see Figure 4 and Figure 5 for an explanation of this notation. The (n+1)-th column of $\boldsymbol{X}_{ij}$ is replaced with the first column of $\boldsymbol{V}_{i,j+1}$, and the (m+1)-th row of $\boldsymbol{X}_{ij}$ is replaced with the first row of $\boldsymbol{V}_{i+1,j}$. That is, the algorithm replaces the mismatched overlapping portions of $\boldsymbol{X}_{ij}$ with the corresponding portions of its neighboring subpatterns $\boldsymbol{V}_{i,j+1}$, $\boldsymbol{V}_{i,j-1}$, $\boldsymbol{V}_{i+1,j}$, or $\boldsymbol{V}_{i-1,j}$, which are the results of the recall process of the corresponding subnetworks. After the replacement, the subnetwork goes through the recall process again and examines the number of mismatches of the resultant subpattern. If the number of resultant mismatched portions is smaller than the previous one, the algorithm keeps this modified result. If the number of mismatched portions is not smaller than the previous one, the previous result $\boldsymbol{V}_{ij}$ is kept. Then, the marker moves horizontally to the next subnetwork. After the marker returns to the initial subnetwork, it then moves vertically to the next row and repeats the same procedure for the new row. Note that the next row of the p-th row of the pattern shown in Figure 4 is its first row. The error correction stage is finished when the marker returns to the subnetwork that the marker initially started from. We can repeat the error correction algorithm so that the subpatterns can go through the error correction stage multiple times.

The main idea behind the error correction algorithm is to replace the incorrectly recalled elements of the subpattern with the ones from the neighboring subpatterns and let the modified subpattern go through the recall process again. If the elements from the neighboring subpatterns are correctly recalled, it is more probable that the current subpattern will be recalled correctly at the error correction stage. The reason is that we might have reduced the number of entries with errors and put the subpattern in the basin of attraction of the prototype subpattern by replacing the overlapping elements.

C. Storing and retrieving images

We simulated neural associative memory system described above using 150×150 pixel gray scale images as patterns. The pixels of original images were represented with 8 bits. To reduce the computational load, we carried

Fig. 6: Quantized prototype gray scale image patterns.

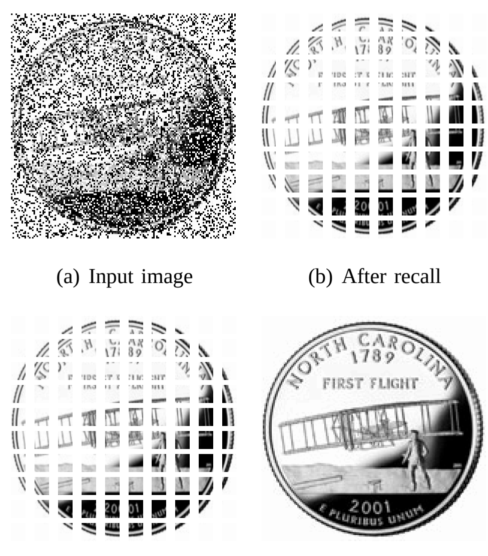

(a) Input image (b) After recall

(c) After error correction (d) Output image

Fig. 7: An example of a gray scale image retrieval using the gBSB-based large scale associative memory.

Fig. 8: Quantized prototype color image patterns with 12 bits/pixel.

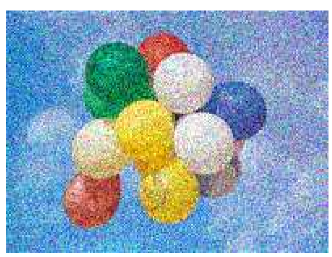

(a) Input image

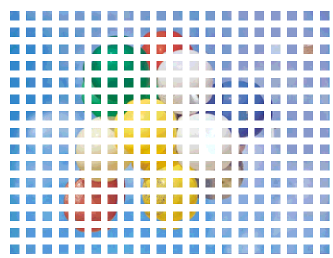

(b) Result after recall process

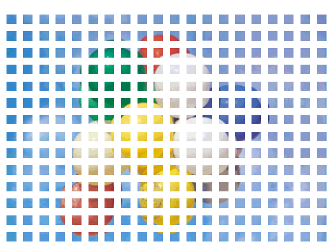

(c) Result after error correction process

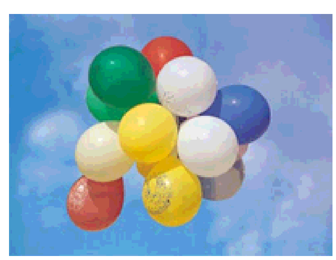

(d) Output image

Fig. 9: Simulation result of image retrieval using the gBSB-based large scale associative memory with color images.

out the uniform quantization so that the quantized images could be represented with 6 bits per pixel. The number of levels of the original image is $2^8 = 256$, and that of the quantized image is $2^6 = 64$. The simplest way of uniform quantization would be to divide the range $[0, 255]$ using 64 intervals of the same length and assign a binary number with 6 digits to each interval. In this paper, we used a slightly different way to quantize images. Instead of dividing the range $[0, 255]$ into the intervals of the same length, we allocated the same length to the inner intervals and we assigned half the length of them to two outermost intervals. The reason why we used this scheme is because the processed images had many pixels with extreme values, i.e. 0 and 255. The quantized image patterns are shown in Figure 6.

An example result of the image recall with the gBSB neural networks is shown in Figure 7. The input image in Figure 7(a) is a noisy version of a stored image pattern. The noise in this image is a so called 'salt-and-pepper noise' with error probability of 0.5. In other words, each pixel might be corrupted by a noise with probability 0.5, and this noisy pixel is white or black with the same probability. The input image was quantized employing the same method as was used for the stored image patterns. The whole image pattern was decomposed into $100\,(10 \times 10)$ subpatterns using the overlapping decomposition method described previously. Each subpattern went through the recall process of the corresponding subnetwork. The result after the recall processes of all the subnetworks is shown in Figure 7(b). There were 5 mismatched portions between subpatterns in this example. The next stage was the error correction process. The collection of sub-images in Figure 7(c) is the result of error correction process. There was no mismatched portion between these subpatterns. Finally, the reconstructed image is shown in Figure 7(d). In this image, there was no erroneously reconstructed pixel out of $22500\,(150 \times 150)$ pixels, that is, no pixel in the reconstructed image had different values from the corresponding stored prototype image. More simulation results involving prototype patterns of Figure 6 can be found in [33].

We can apply the same procedure to the recall of color images. We tested the procedure on color images shown in Figure 8. The pixels in the original images were represented by 24 bits (8 bits for each of the R,G,B components) before the uniform quantization preprocessing. The image patterns in Figure 8 are the quantized versions of the original images with 12 bits per pixel (4 bits for each of the R,G,B components). An example of a simulation result is shown in Figure 9. The size of images used in this simulation was 150×200 pixels. The noisy input image in Figure 9(a) was generated for the simulation in such a way that each of the three R, G, B matrices were corrupted by zero mean additive Gaussian noise with standard deviation 2. Note that each of the R, G, B elements of each pixel has an integer value in the range $[0, 15]$ in this experiment. The patterns were decomposed into $300\,(= 15 \times 20)$ subpatterns. The number of mismatched portions between subpatterns was 30 after the recall process, and it was reduced to 0 by the subsequent error correction process. The final reconstructed image is shown in Figure 9(d). The number of incorrectly recalled pixels was zero and the prototype image was perfectly reconstructed.

VI. Associative Memory for Pattern Sequence Storage and Retrieval

In this section, we describe a system that can store and retrieve images using associative memory that store and recall pattern sequences.

A. Model

Designing continuous time neural associative memory that can store pattern sequences has been investigated in [34], [35], [36], [37], [38], [39]. The discrete time neural models for storage and recollection of pattern sequences can be found in [40], [41], [42], [43], [44]. We first propose a gBSB-based hybrid neural model that can store and recall pattern sequences and then use this network to effectively store and retrieve images.

Suppose that we wish to store a sequence of patterns $\boldsymbol{v}_1, \boldsymbol{v}_2, \ldots, \boldsymbol{v}_L$ in the neural memory in the given order. Following Lee [39], we represent the sequence of patterns above as $\boldsymbol{v}_1 \to \boldsymbol{v}_2 \to \boldsymbol{v}_3 \to \cdots \to \boldsymbol{v}_L$ to make the order of patterns clear. It is easy to show that a neural system described by the following equation can achieve the storage and retrieval of the pattern sequence,

$$\boldsymbol{x}(k+1) = \boldsymbol{W}_h \boldsymbol{x}(k), \tag{10}$$

where the weight matrix $\boldsymbol{W}_h$ has the form,

$$\boldsymbol{W}_h = \boldsymbol{V}_2 \boldsymbol{V}_1^{\dagger}, \tag{11}$$

where

$$\boldsymbol{V}_1 = \begin{bmatrix} \boldsymbol{v}_1 & \boldsymbol{v}_2 & \boldsymbol{v}_3 & \cdots & \boldsymbol{v}_{L-1} \end{bmatrix} \tag{12}$$

and

$$\boldsymbol{V}_2 = \begin{bmatrix} \boldsymbol{v}_2 & \boldsymbol{v}_3 & \boldsymbol{v}_4 & \cdots & \boldsymbol{v}_L \end{bmatrix}. \tag{13}$$

Indeed, suppose that the pattern vectors $\boldsymbol{v}_1, \boldsymbol{v}_2, \boldsymbol{v}_3, \ldots, \boldsymbol{v}_{L-1} \in \{-1,1\}^n$ are linearly independent and $n \geq L-1$. In other words, $\boldsymbol{V}_1 \in \{-1,1\}^{n\times(L-1)}$ and rank $\boldsymbol{V}_1 = L-1$. Then, the pseudo-inverse matrix of $\boldsymbol{V}_1$ is equal to the left pseudo-inverse matrix of $\boldsymbol{V}_1$ [45, page 207], that is,

$$\boldsymbol{V}_1^{\dagger} = (\boldsymbol{V}_1^T \boldsymbol{V}_1)^{-1} \boldsymbol{V}_1^T. \tag{14}$$

Note that

$$\begin{aligned} \boldsymbol{W}_h \boldsymbol{V}_1 &= \boldsymbol{V}_2 \boldsymbol{V}_1^{\dagger} \boldsymbol{V}_1 \\ &= \boldsymbol{V}_2 (\boldsymbol{V}_1^T \boldsymbol{V}_1)^{-1} \boldsymbol{V}_1^T \boldsymbol{V}_1 \\ &= \boldsymbol{V}_2. \end{aligned}$$

Therefore,

$$\boldsymbol{W}_h \boldsymbol{v}_i = \boldsymbol{v}_{i+1}, \quad i = 1, 2, \ldots, L-1.$$

Thus, the system (10) generates the output patterns $\boldsymbol{v}_2, \boldsymbol{v}_3, \ldots, \boldsymbol{v}_L$ for $k = 1, 2, \ldots, L-1$ in a sequential manner for the initial input $\boldsymbol{x}(0) = \boldsymbol{v}_1$. Therefore, we can store a sequence of patterns by constructing the weight matrix $\boldsymbol{W}_h$ using (11), and retrieve the whole sequence when a noiseless stored initial pattern is submitted as an initial condition to the neural system (10).

In the case when there are more than one sequence of patterns to store, we can determine the matrices $\boldsymbol{V}_1$ and $\boldsymbol{V}_2$ using the same idea as above. Assume that there are M sequences of patterns to store,

$$\begin{array}{ccccccc} \boldsymbol{v}_1^{(1)} & \to & \boldsymbol{v}_2^{(1)} & \to & \cdots & \to & \boldsymbol{v}_{L_1}^{(1)}, \\ \boldsymbol{v}_1^{(2)} & \to & \boldsymbol{v}_2^{(2)} & \to & \cdots & \to & \boldsymbol{v}_{L_2}^{(2)}, \\ & \cdots & & \cdots & & \cdots & \\ \boldsymbol{v}_1^{(M)} & \to & \boldsymbol{v}_2^{(M)} & \to & \cdots & \to & \boldsymbol{v}_{L_M}^{(M)}. \end{array}$$

Then, the matrices $\boldsymbol{V}_1$ and $\boldsymbol{V}_2$ have the following forms,

$$\begin{aligned} \boldsymbol{V}_1 = \Big[& \boldsymbol{v}_1^{(1)} \quad \boldsymbol{v}_2^{(1)} \quad \cdots \quad \boldsymbol{v}_{L_1-1}^{(1)} \\ & \vdots \quad \cdots \quad \vdots \quad \boldsymbol{v}_1^{(M)} \quad \boldsymbol{v}_2^{(M)} \quad \cdots \quad \boldsymbol{v}_{L_M-1}^{(M)} \Big] \end{aligned} \tag{15}$$

and

$$\begin{aligned} \boldsymbol{V}_2 = \Big[& \boldsymbol{v}_2^{(1)} \quad \boldsymbol{v}_3^{(1)} \quad \cdots \quad \boldsymbol{v}_{L_1}^{(1)} \\ & \vdots \quad \cdots \quad \vdots \quad \boldsymbol{v}_2^{(M)} \quad \boldsymbol{v}_3^{(M)} \quad \cdots \quad \boldsymbol{v}_{L_M}^{(M)} \Big]. \end{aligned} \tag{16}$$

The number of patterns in each sequence may be different from each other. Hence, if $k \geq L_i, i = 1, 2, \ldots, M$, the neural system (10) might give unexpected outputs. To prevent this, we modify (15) and (16) as follows:

$$\begin{aligned} \boldsymbol{V}_1 = \Big[& \boldsymbol{v}_1^{(1)} \ \boldsymbol{v}_2^{(1)} \ \cdots \ \boldsymbol{v}_{L_1-1}^{(1)} \ \boldsymbol{v}_{L_1}^{(1)} \\ & \vdots \cdots \vdots \ \boldsymbol{v}_1^{(M)} \ \boldsymbol{v}_2^{(M)} \ \cdots \ \boldsymbol{v}_{L_M-1}^{(M)} \ \boldsymbol{v}_{L_M}^{(M)} \Big] \end{aligned} \tag{17}$$

and

$$\boldsymbol{V}_2 = \Big[\boldsymbol{v}_2^{(1)} \; \boldsymbol{v}_3^{(1)} \; \cdots \; \boldsymbol{v}_{L_1}^{(1)} \; \boldsymbol{v}_1^{(1)} \\ \vdots \cdots \vdots \; \boldsymbol{v}_2^{(M)} \; \boldsymbol{v}_3^{(M)} \; \cdots \; \boldsymbol{v}_{L_M}^{(M)} \; \boldsymbol{v}_1^{(M)} \Big]. \quad (18)$$

In this case, the neural system yields the output of the circular pattern sequence,

$$\boldsymbol{v}_1^{(i)} \to \boldsymbol{v}_2^{(i)} \to \cdots \to \boldsymbol{v}_{L_i}^{(i)} \\ \to \boldsymbol{v}_1^{(i)} \to \boldsymbol{v}_2^{(i)} \to \cdots \to \boldsymbol{v}_{L_i}^{(i)} \to \boldsymbol{v}_1^{(i)} \cdots .$$

The above model works well in the case when there is no noise in the initial pattern, but it may not work well with a noisy initial pattern. To overcome this noise problem, we propose a system whose dynamics are described as follows:

$$\begin{aligned} \boldsymbol{x}(k+1) &= \boldsymbol{g}\{(1-c(k))((\boldsymbol{I}_n + \alpha \boldsymbol{W}_a)\boldsymbol{x}(k) + \alpha \boldsymbol{b}) \\ &\quad + c(k)\boldsymbol{W}_h \boldsymbol{x}(k)\}, \end{aligned} \quad (19)$$

$$c(k) = \begin{cases} 1 & \text{if} \quad k = jp-1, \; k > 0, \\ 0 & \text{if} \quad k \neq jp-1, \end{cases} \quad (20)$$

where $k = 0, 1, 2, 3, \ldots$, $j = 0, 1, 2, 3, \ldots$, p is a fixed positive integer, and initial condition $\boldsymbol{x}(0) = \boldsymbol{x}_0$, The activation function $\boldsymbol{g}$, the step size α, and the bias vector $\boldsymbol{b}$ are the same as defined in previous sections. There are two different weight matrices, $\boldsymbol{W}_a$ and $\boldsymbol{W}_h$ in (19). The weight matrix $\boldsymbol{W}_a$ is for autoassociation. The synthesis of the weight matrix $\boldsymbol{W}_a$ and the construction of the bias vector $\boldsymbol{b}$ follow the algorithm described in Section IV. The weight matrix $\boldsymbol{W}_h$ is for heteroassociation. That is, the transition from one pattern to another is achieved by $\boldsymbol{W}_h$. The design of $\boldsymbol{W}_h$ follows the method described above in this section. The role of the function $c(k)$ in (19) is to regulate the timing of pattern transitions. When $c(k) = 0$, the proposed model acts as a gBSB neural network, which is an autoassociative neural system, and when $c(k) = 1$, it works as a heteroassociative one. The transition is set to occur periodically with a period p as specified by (20).

When an initial pattern is presented to the neural system (19), it acts as a gBSB neural system when $k < p$. If the initial pattern is located in the basin of attraction of a stored pattern, the network trajectory moves toward the stored pattern as k increases while $k < p$. In other words, $\{\boldsymbol{x}(0), \boldsymbol{x}(1), \boldsymbol{x}(2), \ldots, \boldsymbol{x}(p-1)\}$ forms a trajectory that approaches a prototype super stable equilibrium state. At $k = p$, the transition to the next pattern occurs. If the trajectory reaches the stored prototype pattern while $k < p$, the transition at $k = p$ gives the next stored pattern of the sequence exactly. In this case, noise was eliminated by the network and the neural system can retrieve the exact stored pattern sequence after $k = p$ with p repetitions of the same pattern. In other words, if $\boldsymbol{x}(p-1) = \boldsymbol{v}_1^{(i)}$, where $\boldsymbol{v}_1^{(i)}$ is the first pattern in the i-th stored pattern sequence, we obtain

$$\boldsymbol{x}(p) = \boldsymbol{x}(p+1) = \boldsymbol{x}(p+2) = \\ \ldots = \boldsymbol{x}(2p-1) = \boldsymbol{v}_2^{(i)}, \\ \boldsymbol{x}(2p) = \boldsymbol{x}(2p+1) = \boldsymbol{x}(2p+2) = \\ \ldots = \boldsymbol{x}(3p-1) = \boldsymbol{v}_3^{(i)},$$

and so on. Consider the case when the initial pattern does not reach the first stored pattern for $k < p$, that is, $\boldsymbol{x}(p-1) \neq \boldsymbol{v}_1^{(i)}$. Then, $\boldsymbol{x}(p) \neq \boldsymbol{v}_2^{(i)}$. In other words, $\boldsymbol{x}(p)$ is still noisy. But, if $\boldsymbol{x}(p)$ is in the basin of attraction of $\boldsymbol{v}_2^{(i)}$, the trajectory approaches $\boldsymbol{v}_2^{(i)}$ as k increases while $p \leq k < 2p$ because now the neural system works as an autoassociative system for this period. If the trajectory reaches a prototype pattern $\boldsymbol{v}_2^{(i)}$, the pattern sequence can be retrieved without noise. In summary, if $\boldsymbol{x}(k)$ is noisy, the noise elimination process by the autoassociative part of the system and the transition to the next pattern by the heteroassociative part will continue alternately until noise is eliminated.

We can modify the above system to speed up the retrieval process. There exist $p-1$ redundant patterns in every p output patterns after the pattern sequence reaches one of the prototype pattern. We can modify the function $c(k)$ in (20) to eliminate the redundant patterns from the output sequence. Once $\boldsymbol{x}(k)$ reaches the prototype pattern, the autoassociative iterations will not change it again and the heteroassociative part alone can retrieve the pattern sequence successfully in the subsequent iterations. This can be done by setting $c(k) = 1$ and fixing it after $\boldsymbol{x}(k)$ reaches the prototype pattern. We summarize the above consideration in the following algorithm.

Algorithm 6.1: Algorithm to eliminate redundant autoassociative iterations in pattern sequence recall

1. Set $flag = 0$.

2. Set $k = 0$.

3. while $flag = 0$

3.1. If $k \neq jp-1$, set $c(k) = 0$. If $k = jp-1$, set $c(k) = 1$.

3.2. Calculate

$$\begin{aligned} \boldsymbol{x}(k+1) &= \boldsymbol{g}\{(1-c(k))((\boldsymbol{I}_n + \alpha \boldsymbol{W}_a)\boldsymbol{x}(k) + \alpha \boldsymbol{b}) \\ &\quad + c(k)\boldsymbol{W}_h \boldsymbol{x}(k)\}. \end{aligned}$$

3.3. If $\boldsymbol{x}(k+1) = \boldsymbol{x}(k)$, set $flag = 1$.

3.4. Set $k = k+1$.

4. Set $c(k) = 1$ and calculate

$$\begin{aligned} \boldsymbol{x}(k+1) &= \boldsymbol{g}\{(1-c(k))((\boldsymbol{I}_n + \alpha \boldsymbol{W}_a)\boldsymbol{x}(k) + \alpha \boldsymbol{b}) \\ &\quad + c(k)\boldsymbol{W}_h \boldsymbol{x}(k)\} \end{aligned}$$

for the subsequent iterations.

Example 6.1 The example of pattern sequence retrieval using the above algorithm is shown in Figures 10 and 11.

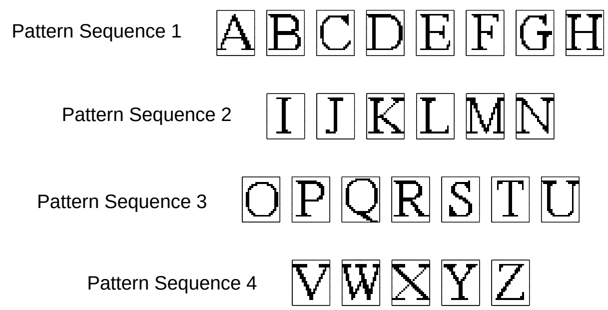

Fig. 10: Prototype pattern sequences for Example 6.1.

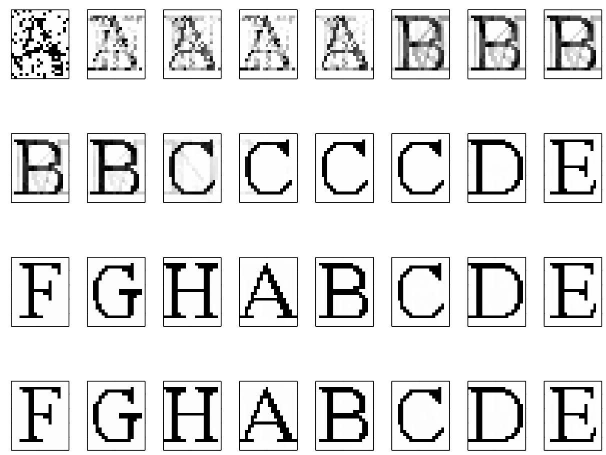

Fig. 11: Snapshots of the pattern sequence recall in Example 6.1: the proposed hybrid neural model with a noisy initial pattern.

B. Storing and retrieving images

In this section, we describe a gBSB-based neural system that can store and retrieve images using the neural system described in Section VI-A and the concept of image decomposition. Suppose we have M images to store in the neural memory. First, each prototype image that we wish to store is decomposed into equal-sized sub-images, $s_1^{(i)}, s_2^{(i)}, \ldots, s_L^{(i)}$, where $i = 1, 2, \ldots, M$. Then, we represent each sub-image $s_l^{(i)}$ as a binary vector $\boldsymbol{v}_l^{(i)}$. Treating the binary vectors $\boldsymbol{v}_1^{(i)}, \boldsymbol{v}_2^{(i)}, \ldots, \boldsymbol{v}_L^{(i)}$ as a pattern sequence $\boldsymbol{v}_1^{(i)} \rightarrow \boldsymbol{v}_2^{(i)} \rightarrow \cdots \rightarrow \boldsymbol{v}_L^{(i)}$, we construct a neural associative memory as proposed in

Section VI-A.

When a noisy image is presented to the network, it is first decomposed into L equal-sized sub-images and they are converted into binary vectors. Then, they form a sequence of vectors to be processed by the neural system and enter into the stage of the pattern sequence retrieval. The autoassociative iterations are eliminated at some point and only heteroassociative steps are necessary thereafter. Note that the pattern sequence retrieval is carried out in reverse order of sequence formation. Once a complete pattern sequence is retrieved, the patterns included in the sequence are converted back into images. Finally, we combine those sub-images to obtain the original image with the same size as before its decomposition.

We present the snapshots of the simulation result in Figure 12. The size of image used in this experiment is 160×120 and each pixel was represented by a binary number of 8 bits to give gray level range $[0, 255]$. The image was decomposed into 48 sub-images where each sub-image is a 20×20 gray scale image. Those 48 sub-images form a pattern sequence. Then, the neural system proposed above was constructed to store the prototype images. In this experiment, we added zero mean Gaussian noise with standard deviation 30 to the value of each pixel of the prototype image to get an input image. The input image is shown in Figure 12 (a). This image was decomposed into 48 sub-images and the image reconstruction started with the autoassociative recall of the fist sub-image. The number p was set to $p = 10$. As we can see in Figure 12 (b), the first sub-image did not converge to the corresponding prototype sub-image by $k = 9$. Because we set $p = 10$, the heteroassociative step occurred at $k = 10$, which is shown in Figure 12 (c). Then, autoassociative iterations were carried out in the second sub-image. Because the second sub-image did not converge to the corresponding prototype sub-image until $k = 19$ (Figure 12 (d)), the heteroassociative recall occurred at $k = 20$ (Figure 12 (e)). The third sub-image converged to the prototype sub-image at $k = 25$ with the autoassociative recall (Figure 12 (f)). Then, $c(k)$ was set as $c(k) = 1$ so that the redundant autoassociative iterations are not performed in the subsequent recall process. From $k = 26$, the recall process was performed with only heteroassociative steps and it stopped at $k = 72$. The reconstructed image is shown in Figure 12 (l). Note that the recall of the last sub-image was done at $k = 70$ (Figure 12 (j)) but the recall process continued to complete the recall of the first and the second sub-images, which was not completed during the previous pass (Figure 12 (b), Figure 12 (d)). It continued to $k = 72$ to complete the recall (Figure 12 (k), Figure 12 (l)). Perfect recall occurred and we successfully reconstructed the prototype image.

VII. Conclusions

In this paper, we first reviewed some properties of the gBSB neural model that make this network suitable for using it in constructing associative memories. We employed the gBSB networks as building blocks in two different types of associative memory structures that can store and retrieve images. Both networks use pattern decomposition. By using pattern decomposition, we were able to reduce the computational load for processing images. In the first network, an error correction feature was added to the system to enhance the recall performance of the neural memory. In the second system, the concept of pattern sequence storage and retrieval was used. Because the autoassociative iteration step can be eliminated after some number of iterations, this method further reduces the computation load.

VIII. Further Research

We are investigating the problem of identification of the parameters of an autoregressive (AR) time series

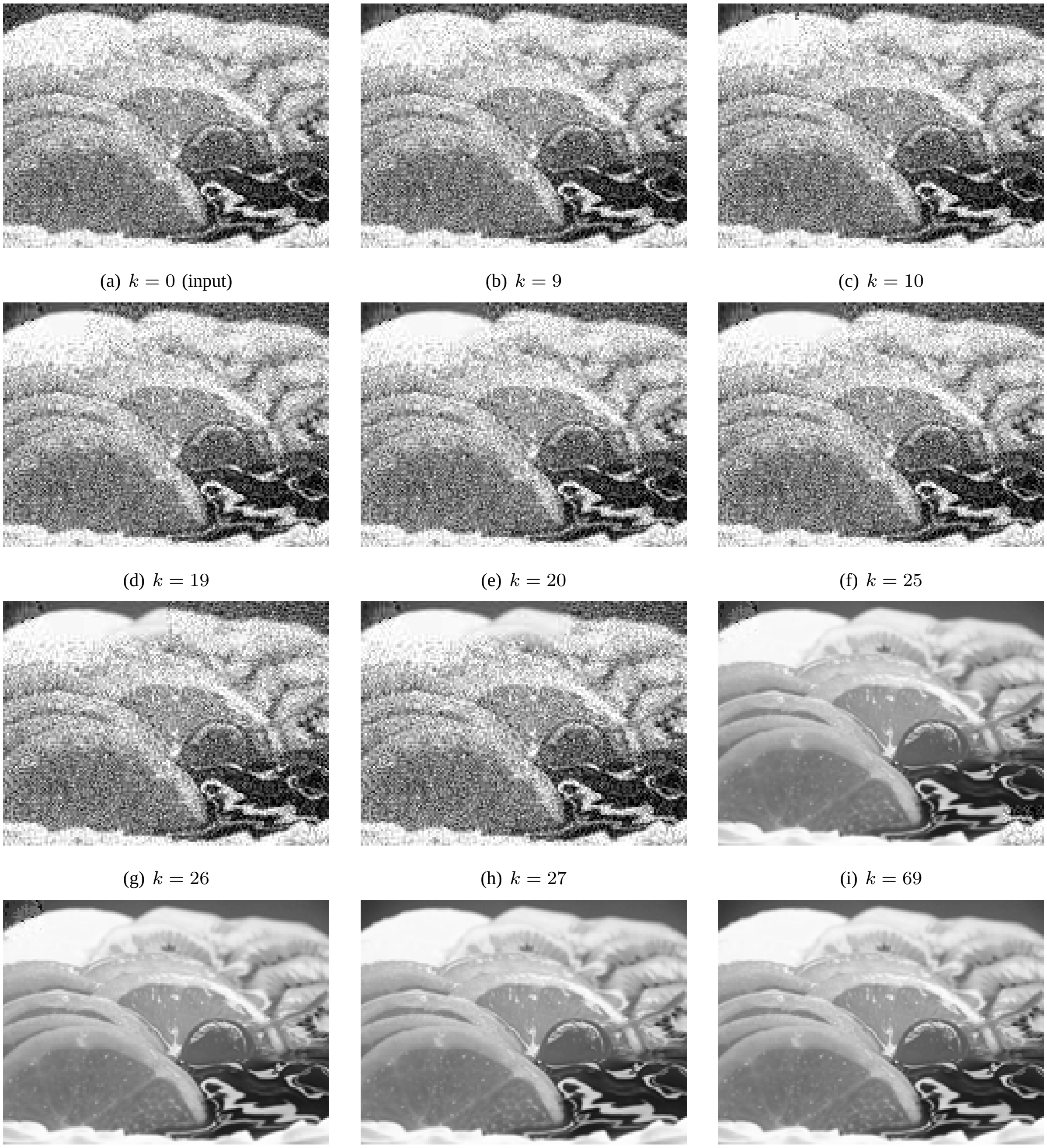

(a) $k = 0$ (input) (b) $k = 9$ (c) $k = 10$

(d) $k = 19$ (e) $k = 20$ (f) $k = 25$

(g) $k = 26$ (h) $k = 27$ (i) $k = 69$

(j) $k = 70$ (k) $k = 71$ (l) $k = 72$ (output)

Fig. 12: Snapshots of the recall process of the proposed neural system. (Input image is a noisy version of the prototype image corrupted by the Gaussian noise.)

model using the gBSB net. The parameters of the model are determined so that the sum of square errors between the values of the estimated terms and the actual terms is minimized. This method is based on the fact that each trajectory of the gBSB neural model progresses to the local minimizer of the energy function of the neural net. The gBSB neural net is designed so that the energy function of the network is the same as the error function that is to be minimized. In this particular procedure, the energy function of the neural network is convex, which implies that any local minimizer found by the gBSB algorithm must actually be a global minimizer. Using the above preliminary results, we are developing an algorithm for estimating the time series parameters. The algorithm can then be employed to analyze myoelectric signals. This method of analyzing myoelectric signals can then, in turn, be applied to the control of multi-degree of freedom arm prostheses.

REFERENCES

[1] J. A. Anderson, *An Introduction to Neural Networks*. Cambridge, Massachusetts: A Bradford Book, The MIT Press, 1995.

[2] K. Nakano, "Associatron—a model of associative memory," *IEEE Transactions on Systems, Man, and Cybernetics*, vol. 2, no. 3, pp. 380–388, July 1972.

[3] T. Kohonen, "Correlation matrix memories," *IEEE Transactions on Computers*, vol. 21, no. 4, pp. 353–359, April 1972.

[4] T. Kohonen and M. Ruohonen, "Representation of associated data by matrix operators," *IEEE Transactions on Computers*, vol. 22, no. 7, pp. 701–702, July 1973.

[5] T. Kohonen, "An adaptive associative memory principle," *IEEE Transactions on Computers*, vol. 23, no. 4, pp. 444–445, April 1974.

[6] J. J. Hopfield, "Neural networks and physical systems with emergent collective computational abilities," *Proc. Natl. Acad. Sci. USA, Biophysics*, vol. 79, pp. 2554–2558, April 1982.

[7] B. Kosko, "Adaptive bidirectional associative memories," *Applied Optics*, vol. 26, no. 23, pp. 4947–4960, December 1987.

[8] P. Kanerva, *Sparse Distributed Memory*. Cambridge, Mass.: MIT Press, 1988.

[9] J. A. Anderson, J. W. Silverstein, S. A. Ritz, and R. S. Jones, "Distinctive features, categorical perception, probability learning: Some applications of a neural model," in *Neurocomputing; Foundations of Research*, J. A. Anderson and E. Rosenfeld, Eds. Cambridge, MA: The MIT Press, 1989, ch. 22, pp. 283–325, reprint from *Psychological Review* 1977, vol. 84, pp. 413–451.

[10] A. Schultz, "Collective recall via the Brain-State-in-a-Box network," *IEEE Transactions on Neural Networks*, vol. 4, no. 4, pp. 580–587, July 1993.

[11] H. J. Greenberg, "Equilibria of the Brain-State-in-a-Box (BSB) neural model," *Neural Networks*, vol. 1, no. 4, pp. 323–324, 1988.

[12] R. M. Golden, "The "Brain-State-in-a-Box" neural model is a gradient descent algorithm," *Journal of Mathematical Psychology*, vol. 30, no. 1, pp. 73–80, 1986.

[13] ——, "Stability and optimization analyses of the generalized Brain-State-in-a-Box neural network model," *Journal of Mathematical Psychology*, vol. 37, no. 2, pp. 282–298, 1993.

[14] S. Grossberg, "Nonlinear neural networks: Principles, mechanisms, and architectures," *Neural Networks*, vol. 1, no. 1, pp. 17–61, 1988.

[15] S. Hui and S. H. Żak, "Dynamical analysis of the Brain-State-in-a-Box (BSB) neural models," *IEEE Transactions on Neural Networks*, vol. 3, no. 1, pp. 86–94, January 1992.

[16] F. Hakl, "Recall strategy of B-S-B neural network," *Neural Network World*, vol. 2, no. 1, pp. 59–82, 1992.

[17] S. Hui, W. E. Lillo, and S. H. Żak, "Dynamics and stability analysis of the Brain-State-in-a-Box (BSB) neural models," in *Associative Neural Memories; Theory and Implementation*, M. H. Hassoun, Ed. New York: Oxford University Press, 1993, ch. 11, pp. 212–224.

[18] W. E. Lillo, D. C. Miller, S. Hui, and S. H. Żak, "Synthesis of Brain-State-in-a-Box (BSB) based associative memories," *IEEE Transactions on Neural Networks*, vol. 5, no. 5, pp. 730–737, 1994.

[19] R. Perfetti, "A synthesis procedure for Brain-State-in-a-Box neural networks," *IEEE Transactions on Neural Networks*, vol. 6, no. 5, pp. 1071–1080, September 1995.

[20] M. H. Hassoun, *Fundamentals of Artificial Neural Networks*. Cambridge, MA: A Bradford Book, The MIT Press, 1995.

[21] S. H. Żak, W. E. Lillo, and S. Hui, "Learning and forgetting in generalized Brain-State-in-a-Box (BSB) neural associative memories," *Neural Networks*, vol. 9, no. 5, pp. 845–854, July 1996.

[22] H. Y. Chan and S. H. Żak, "On neural networks that design neural associative memories," *IEEE Transactions on Neural Networks*, vol. 8, no. 2, pp. 360–372, March 1997.

[23] ——, "Real-time synthesis of sparsely interconnected neural associative memories," *Neural Networks*, vol. 11, no. 4, pp. 749–759, June 1998.

[24] J. Park, H. Cho, and D. Park, "Design of GBSB neural associative

memories using semidefinite programming," *IEEE Transactions on Neural Networks*, vol. 10, no. 4, pp. 946–950, July 1999.

[25] J. Li, A. N. Michel, and W. Porod, "Analysis and synthesis of a class of neural networks: Linear systems operating on a closed hypercube," *IEEE Transactions on Circuits and Systems*, vol. 36, no. 11, pp. 1405–1422, 1989.

[26] S. H. Żak, *Systems and Control*. New York: Oxford University Press, 2003.

[27] J. Park and Y. Park, "An optimization approach to design of generalized BSB neural associative memories," *Neural Computations*, vol. 12, no. 6, pp. 1449–1462, 2000.

[28] F. Sevrani and K. Abe, "On the synthesis of Brain-State-in-a-Box neural models with application to associative memory," *Neural Computation*, vol. 12, no. 2, pp. 451–472, February 2000.

[29] C. Zetzsche, "Sparse coding: the link between low level vision and associative memory," in *Parallel Processing in Neural Systems and Computers*, R. Eckmiller, G. Hartmann, and G. Hauske, Eds. Amsterdam, The Netherlands: Elsevier Science Publishers B. V. (North-Holland), 1990, pp. 273–276.

[30] N. Ikeda, P. Watta, M. Artiklar, and M. H. Hassoun, "A two-level Hamming network for high performance associative memory," *Neural Networks*, vol. 14, no. 9, pp. 1189–1200, November 2001.

[31] M. Akar and M. E. Sezer, "Associative memory design using overlapping decompositions," *Automatica*, vol. 37, no. 4, pp. 581–587, April 2001.

[32] C. Oh and S. H. Żak, "Associative memory design using overlapping decomposition and generalized Brain-State-in-a-Box neural networks," *International Journal of Neural Systems*, vol. 13, no. 3, pp. 139–153, June 2003.

[33] ——, "Image recall using large scale generalized Brain-State-in-a-Box neural network," *International Journal of Applied Mathematics and Computer Science*, vol. 15, no. 1, pp. 99–114, March 2005.

[34] H. Sompolinsky and I. Kanter, "Temporal association in asymmetric neural networks," *Physical Review Letters*, vol. 57, no. 22, pp. 2861–2864, December 1986.

[35] Y. Baram, "Memorizing binary vector sequences by a sparsely encoded network," *IEEE Transactions on Neural Networks*, vol. 5, no. 6, pp. 974–981, November 1994.

[36] M. Morita, "Associative memory with nonmonotone dynamics," *Neural Networks*, vol. 6, no. 1, pp. 115–126, 1993.

[37] ——, "Smooth recollection of a pattern sequence by nonmonotone alalog neural networks," in *Proceedings of the IEEE International Conference on Neural Networks*, vol. 2, June 27–July 2, 1994, pp. 1032–1037.

[38] ——, "Memory and learning of sequential patterns by nonmonotone neural networks," *Neural Networks*, vol. 9, no. 8, pp. 1477–1489, November 1996.

[39] D.-L. Lee, "Pattern sequence recognition using a time-varying Hopfield network," *IEEE Transactions on Neural Networks*, vol. 13, no. 2, pp. 330–342, March 2002.

[40] L. Personnaz, I. Guyon, and G. Dreyfus, "Collective computational properties of neural networks: New learning mechanisms," *Physical Review A*, vol. 34, no. 5, pp. 4217–4228, November 1986.

[41] I. Guyon, L. Personnaz, J. P. Nadal, and G. Dreyfus, "Storage and retrieval of complex sequences in neural networks," *Physical Review A*, vol. 38, no. 12, pp. 6365–6372, December 1988.

[42] R. W. Zhou and C. Quek, "DCBAM: a discrete chainable bidirectional associative memory," *Pattern Recognition Letters*, vol. 17, pp. 985–999, 1996.

[43] D.-L. Lee, "A discrete sequential bidirectional associative memory for multistep pattern recognition," *Pattern Recognition Letters*, vol. 19, pp. 1087–1102, 1998.

[44] L. Wang, "Heteroassociations of spatio-temporal sequences with the bidirectional associative memory," *IEEE Transactions on Neural Networks*, vol. 11, no. 6, pp. 1503–1505, November 2000.

[45] E. K. P. Chong and S. H. Żak, *An Introduction to Optimization*, 2nd ed. New York: Wiley-Interscience, John Wiley & Sons, Inc., 2001.